Hydrogen Effect on Atomic Configuration of keV-Ion-Irradiated Carbon

G. Compagnini, L. Calcagno, and G. Foti

Dipartimento di Fisica, Università di Catania, Corso Italia 57-195129, Catania, Italy
(Received 22 January 1992)

The structure of ion-irradiated hydrogenated amorphous carbon and hydrogenated graphitic carbon films has been investigated by measuring the trigonal carbon fraction by optical measurements and the hydrogen concentration by elastic recoil of 2.0-MeV He^+ ions. After irradiation both graphitic and amorphous carbon samples showed a unique relationship between the trigonal bonded carbon and the hydrogen fraction, regardless of the original film structure.

Amorphous carbon films have attracted increasing interest for both scientific and technological reasons [1-5]. From a technological point of view they have unique physical and chemical properties (hardness, optical transparency, chemical inertness) and can be adopted as protective antireflective films and as coatings [1,2]. Moreover the ability of carbon to have threefold or fourfold coordination deserves a lot of interest from the theoretical point of view, and although there have been many investigations, the characteristic properties of these materials are largely unknown and the subject of controversy [6-9].

It is known that carbon atoms show two different bonding configurations, namely, sp^3 and sp^2. In the first one, each of the four valence electrons is assigned to tetrahedrally directed sp^3 hybrid orbitals which make a strong σ bond with one adjacent atom. In the sp^2 configuration, three of the four electrons are assigned to trigonal sp^2 hybrid orbitals which again form σ bonds, while the fourth electron is directed normally to the σ bonding plane and generates weak delocalized π bonds. The theoretical characterization is very hard because it is difficult to construct a suitable interatomic potential for these bonds; however, Galli *et al.* performed calculations based on a first-principles dynamic method and showed that the more stable configuration of amorphous carbon consists of 85% sp^2 sites and 15% sp^3 sites, where the former are graphitic in nature and the latter are distorted diamond structures [6].

The presence of hydrogen in these structures produces a wide variety of materials with different properties. Hydrogen concentrations in the range (10-35)% give rise to hard (1000-2000 kg/mm^2) hydrogenated amorphous carbon with mixed sp^2 and sp^3 bonding, small energy gaps (0.5-1.5 eV), and high mass densities (1.6-2.2 g/cm^3). Hydrogen contents in the range (35-50)% produce soft material with low density (1-1.6 g/cm^3), high energy gaps (1.5-2.5 eV), and a large density of sp^3 bonds.

Hydrogenated amorphous carbon can be prepared by various techniques such as plasma deposition, sputtering of graphite in a hydrogen-containing atmosphere [10,11], and ion irradiation of hydrocarbon polymers [12]. A strong bond rearrangement is observed in hydrogenated amorphous carbon layers after ion irradiation. The energy transferred from the incident ions to target atoms and/or to the electronic environment produces a cluster-

ing of carbon atoms with the formation of large hexagonal rings as evidenced by the reduction of the energy gap (2.0-0.5 eV).

In this paper we report, for the first time, experimental evidence that the atomic structure of hydrogenated carbon reaches a stable configuration after keV-ion irradiation which depends only on hydrogen content without any memory of initial sample structure (graphite or amorphous).

Hydrogenated amorphous carbon (HAC) layers have been prepared by ion irradiation of polystyrene films with 200-keV C^+ ions swept over a surface area of 1×1 in.^{2} and a beam current of 100 nA for a time of 500 s. These layers were quite transparent with an optical gap of 2.0 eV and a hydrogen atomic concentration of 45%. The polystyrene films were deposited on quartz or silicon substrates by spinning a solution of $CHCl_3$ with a thickness of 300 nm. Some HAC samples were subsequently annealed at 900 °C for 200 s under nitrogen flux to reduce the hydrogen concentration to 10%. After thermal annealing these samples were quite dark with a very low energy gap (below 0.1 eV) and we will refer to them as hydrogenated graphitic carbon (HGC).

Both HAC and HGC sets of samples were then irradiated at room temperature with several ion beams: 250-keV Kr^+, 300-keV Ar^+, 100-keV He^+, and 300-keV H^+ ions in the fluence range 5×10^{14}-1.0×10^{16} ions/cm^2. The ion range was always larger than the sample thicknesses, in order to get uniform irradiated layers.

Trigonal carbon concentrations and the optical energy gaps of these films were measured by optical UV–visible spectrometry, performing transmittance and reflectance measurements with a Lambda 2 Perkin Elmer double-beam spectrometer in the wavelength range 200-1100 nm.

Hydrogen concentrations were measured by the elastic recoil technique [13], using a primary beam of 2.0-MeV helium ions. This technique allows one to obtain hydrogen profiles with a depth resolution of 40 nm and hydrogen concentration down to 1%; moreover it is sensitive to the total amount of hydrogen, bonded as well as unbonded.

As already mentioned, the structure of amorphous carbon is mainly characterized by sp^2 and sp^3 carbon fractions which can be determined by optical investigations.

UV–visible transmittance spectra are reported in Fig. 1(a) for HAC before and after irradiation with 300-keV Ar^+ beams at two different fluences: 2×10^{15} and 5×10^{15} ions/cm^2. In the unirradiated HAC sample, the transmittance spectrum exhibits a typical semiconductor behavior with a high-absorption region in the wavelength range 200–450 nm and a high-transmission region (80%) for wavelengths greater than 700 nm. The absorption edge is located at about 600 nm with a broadening of 200 nm. For ion-irradiated HAC samples a strong reduction in the transmission yield is observed over the entire measured wavelength range, together with a shift of absorption edge toward greater wavelengths. The energy gap, measured with Tauc's procedure [14], depends on ion fluence, going from 2.0 eV for pristine HAC to 0.5 eV for the 5×10^{15}-ions/cm^2-irradiated sample.

Transmittance spectra of HGC are reported in Fig. 1(b) before and after 300-keV Ar^+ irradiation at two different ion fluences: 5×10^{14} and 2×10^{15}/cm^2. In unirradiated HGC samples, the transmission yield is very low (few percent) over the entire wavelength range, while after ion irradiation a strong increase in the high-transmission region is observed up to a factor of 3 for the 2×10^{15}-ions/cm^2 fluence. Moreover the clearing up of the sample agrees with the increase of the energy gap, which goes from less than 0.1 eV for pristine HGC to 0.4 eV for high-fluence-irradiated HGC samples.

The reflectivity spectra show a slow unstructured decrease (from 20% to 10%) with increasing energy due to the smooth variation of the real part of the refractive index. Combining transmittance and reflectance measurements in the investigated wavelength range we have evaluated the atomic fraction of trigonal bonded carbon.
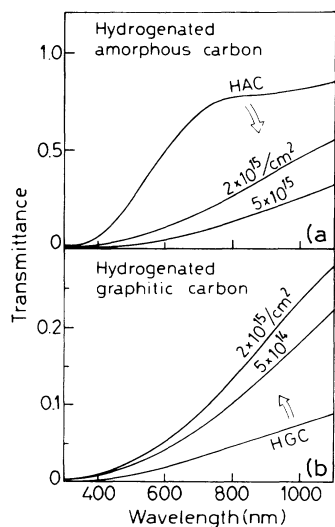
The fit of transmission and reflection spectra allows us to obtain the optical constants n and k and then the imaginary part of dielectric constant $\epsilon_2 = 2nk$, by using a suitable Kramers-Kronig consistent dispersion relation as described elsewhere [15]. Moreover it is well known that the number of effective electrons per atom involved in the interband transitions below the energy E is given by [16]

$$N_{\text{eff}} = (0.766/0.23)(M/\rho)\int_0^E \epsilon_2(E')E'\,dE'$$

where M is the mean atomic mass, E is a suitable energy cutoff, and the factor $1/0.23$ arises from the screening of the π electron system [17]. In the relation (1) $M = x_C A_C + x_H A_H$, where x_C and x_H are the carbon and hydrogen fractions and A_C and A_H their atomic numbers, respectively. Since $\pi \rightarrow \pi^*$ transitions are exhausted at 7 eV, we have used $E = 7$ eV and related the obtained integrated N_{eff} value with that of pure graphite, which is $N_{\text{eff}}^* = 0.83$ in the same energy range.

The trigonal carbon fraction in hydrogenated carbon is given by

$$C_{sp^2} = N_{\text{eff}}/N_{\text{eff}}^* .$$

It must be emphasized that for ion-irradiated carbon the mass density (ρ) and the mean atomic weight (M) change with ion fluence and the change of M is correlated with hydrogen emission from the target. Hydrogen concentration decreases with fluence, following a simple exponential law [12] as $\exp[-\sigma\phi]$, and mass density increases with an exponential relation [18], like $[1 - \exp(-\sigma\phi)]$. For both processes the σ factors are similar within a few percent: For HGC irradiated with 300-keV Ar^+ σ is equal to 5×10^{-16} cm^2, while the saturation values at high ion fluences are $x_H^\infty = 0.18$ and $\rho^\infty = 1.7$ g/cm^2, respectively.

The trigonal carbon fraction (C_{sp^2}) in HAC films was strongly dependent on ion fluence through the change of M, ρ, and ϵ_2 and these were taken into account to calculate C_{sp^2}. The obtained values are reported in Fig. 2(a) versus ion fluence together with hydrogen concentration. C_{sp^2} increases from its initial value of 0.3 following an exponential trend with a saturation value of 0.6 and a cross section of 3.8×10^{-16} cm^2.

Figure 2(b) reports the trigonal carbon fraction for HGC versus ion fluence for 300-keV Ar^+ irradiation; it decreases exponentially from 0.85 to 0.68 with $\sigma = 10^{-15}$ cm^2. In this case the hydrogen concentration is about 10% and does not change with ion fluence.

Irradiations performed with the argon-ion beams on two sets of samples (HAC and HGC) give different saturation values for the trigonal carbon fraction. Then, the final carbon configuration is not only controlled by ion-beam parameters but is related to the initial hydrogen concentration.

In order to test the general correlation between x_H and

FIG. 1. (a) Transmission yield vs wavelength for a pristine HAC sample and for samples irradiated with 300-keV Ar^+ at different fluences. (b) Transmission yield vs wavelength for a pristine HGC sample and for samples irradiated with 300-keV Ar^+ at different fluences.
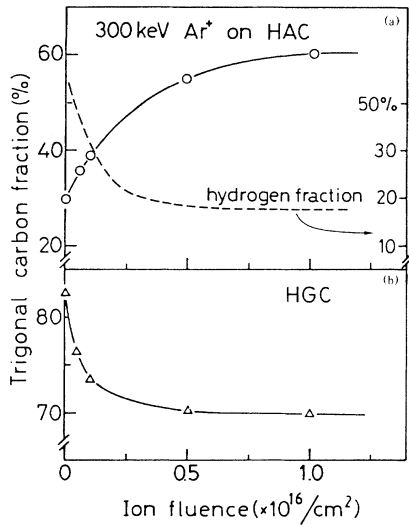
FIG. 2. (a) Trigonal carbon fraction and hydrogen atomic fraction vs ion fluence for 300-keV-Ar$^+$-irradiated HAC samples. (b) Trigonal carbon fraction vs ion fluence for 300-keV-Ar$^+$-irradiated HGC samples.

FIG. 3. Saturation values of trigonal carbon and of hydrogen fraction for different ion-irradiated HAC and HGC samples. On the right ordinate scale the corresponding values of cluster size are reported.

C_{sp^2}, HAC samples have been irradiated with different ion beams: 250-keV Kr$^+$, 100-keV He$^+$, and 300-keV H$^+$. The trend of C_{sp^2} fraction and of hydrogen concentration versus ion fluence is similar to that reported in Fig. 2(a); however, the cross section and the saturation values depend on the ion mass.

In Table I are reported such values together with the total energy loss (S) for each ion; a linear relation holds between cross section and total energy loss. Similar results were obtained for molecular hydrogen release from diamondlike carbon films irradiated by ion beams, where the ion energy release goes to electronic excitations [19].

In our experimental condition for light ions (H$^+$ and He$^+$) the main mechanism of deposited energy is the inelastic interaction with electrons, while for heavy ions, a large fraction of incoming energy goes to elastic interaction with target atoms; however, if we include the effects of secondary recoiled atoms, the fraction of deposited energy through electronic excitation reaches 65% for Kr$^+$ and 80% for Ar$^+$, respectively.

TABLE I. Cross section, energy loss, and saturation values of trigonal carbon percentage, hydrogen percentage, and optical energy gap for different ion-irradiated HAC samples.

Ion and energy	σ $(10^{16}\,cm^2)$	S (eV/Å)	$C_{sp^2}^{\infty}$ (%)	x_H^{∞} (%)	E_g^{∞} (eV)
250-keV Kr	5.5	95	65	16	0.5
300-keV Ar	4.5	80	60	18	0.6
100-keV He	0.8	18	42	30	1.0
300-keV H	0.35	37	8	35	1.1

The saturation values for C_{sp^2} and x_H in both HAC and HGC irradiated samples are reported in Fig. 3, where asterisks refer to the unirradiated samples. All experimental data for keV-ion-irradiated carbon lie on a single curve regardless of the initial sample structure.

As already mentioned, different theoretical models were proposed to describe the structure of carbon systems. Angus and Jansen [9] proposed a random covalent network model and found the following relation between hydrogen concentration and the ratio of tetrahedral to trigonal carbon fraction:

$$C_{sp^3}/C_{sp^2} = (6x_H - 1)/(8 - 13x_H) ,$$

valid for a fully constrained network.

Although there is good agreement for the trigonal carbon fraction in low- and high-hydrogenated films, our experimental points show a large discrepancy in the intermediate hydrogen concentration range ($x_H = 0.5-0.1$). Moreover, Galli et al. [6] showed that the structure of a computer-generated pure amorphous carbon network at 300 K is found to be predominantly graphitic (85% threefold- and 15% fourfold-coordinated carbon atoms).

For ion-irradiated hydrogen-carbon systems a more suitable model seems to be that of Robertson and O'Reilly [7] in which hydrogenated amorphous carbon is considered to consist of sp^2 clusters, typically planar, interconnected by randomly oriented tetrahedrally sp^3 bonds. Unfortunately following this approach it is not possible to obtain one explicit relation between trigonal carbon fraction and hydrogen concentration as for the fully constrained network. However, in this model, the energy gap can be used to give more information on the carbon arrangement inside the film. In fact, since the sp^2 structure is believed to be ordered in benzoid rings, these authors found a relation between the number of benzoid rings inside each cluster (M) and the energy gap:

$E_g = 6/M^{1/2}$. Then HAC, with say $E_g = 1.5$ eV, contains clusters of up to $M = 16$ rings which corresponds to a maximum cluster size of 10 Å. The optical spectra reported in Figs. 1(a) and 1(b) allow us to obtain the value of the optical gap by following the Tauc procedure and the obtained experimental saturation data for HAC irradiated samples are given in Table I. The cluster size estimated from E_g for HAC and HGC samples can be considered as an upper limit for the extension of benzoid rings (see right side of Fig. 3). The broadening in the electronic density of states, corresponding to π and π^* states as detected by photoelectron spectroscopy [20] and optical data [21], suggests a wide cluster size distribution inside our irradiated samples. Although it is very difficult to give a realistic estimation of the cluster size distribution, the trend of the optical gap is still a useful tool to state the cluster size behavior during irradiation.

The final picure that we draw from Fig. 3 is now quite impressive: If we start with hydrogenated graphitic carbon films (E_g below 0.1 eV), keV-ion irradiation produces a strong declustering of atomic configuration of carbon atoms (final $E_g = 0.5$), while for hydrogenated amorphous carbon ion irradiation produces a strong clustering. The equilibrium values of C_{sp^2} fraction depends on hydrogen concentration, which is related to the deposited energy of the incoming ions and to the initial structure of the film.

In summary, ion irradiation of hydrogenated carbon films modifies their physical properties (densities, hydrogen contents, energy gaps, etc.) and the transformation rates are linearly dependent on ion deposited energy. Moreover, a quite realistic picture of atomic carbon configuration is a cluster structure where the final trigonal carbon fraction and cluster size depend on hydrogen concentration.

A general curve (C_{sp^2} vs x_H) for carbon-hydrogen systems was found in such a way that ion irradiation produces declustering if the initial size is larger than the equilibrium value or clustering if it is smaller.

[1] B. Dischler, A. Bubenzer, and P. Koidl, Solid State Commun. 48, 105 (1983).

[2] M. Yoshikowa, G. Katagiri, H. Ishida, A. Ishitani, and T. Akamatsu, Appl. Phys. Lett. 52, 1639 (1988).

[3] T. Datta, J. A. Woollam, and W. Notohaniprodjo, Phys. Rev. B 40, 5956 (1989).

[4] J. Fink, T. Muller-Heinzerling, J. Pluger, A. Bubenzer, P. Koidl, and G. Crecelius, Solid State Commun. 47, 687 (1983).

[5] G. Compagnini, R. Reitano, G. Foti, G. Baratta, and G. Strazzulla, Radiat. Eff. Defects Solids 177, 299 (1991).

[6] G. Galli, R. M. Martin, R. Car, and M. Parrinello, Phys. Rev. Lett. 62, 555 (1989).

[7] J. Robertson and E. P. O'Reilly, Phys. Rev. B 35, 2946 (1987).

[8] D. Beeman, J. Siverman, R. Lynds, and M. R. Anderson, Phys. Rev. B 30, 870 (1984).

[9] J. C. Angus and F. Jansen, J. Vac. Sci. Technol. A 6, 1778 (1988).

[10] J. J. Cuomo, J. P. Doyle, J. Brulev, and J. C. Lin, Appl. Phys. Lett. 58, 466 (1991).

[11] A. Bubenzer, P. Dischler, G. Board, and P. Koidl, J. Appl. Phys. 54, 4590 (1983).

[12] G. Compagnini, G. Foti, R. Reitano, and G. Mondio, Appl. Phys. Lett. 57, 2546 (1990).

[13] B. L. Doyle and P. S. Peercy, Appl. Phys. Lett. 34, 811 (1979).

[14] J. Tauc, in Amorphous and Liquid Semiconductors, edited by J. Tauc (Plenum, London, 1974).

[15] A. R. Forouhy and I. Blommer, Phys. Rev. B 34, 7018 (1986).

[16] F. Wooten, Optical Properties of Solids (Academic, New York, 1972).

[17] E. A. Taft and H. R. Philipp, Phys. Rev. A 138, 197 (1965).

[18] L. Calcagno and G. Foti, Nucl. Instrum. Methods Phys. Res., Sect. B 19/20, 895 (1987).

[19] M. E. Adel, O. Amir, R. Kalish, and L. C. Feldman, J. Appl. Phys. 66, 3248 (1989).

[20] A. Terrasi, G. Foti, Y. Hwu, and G. Margaritondo, J. Appl. Phys. 70, 1885 (1991).

[21] D. Dasgupta, F. Demichelis, C. F. Pirri, and A. Tagliaferro, Phys. Rev. B 43, 2131 (1991).